Engineering and Technology Journal
Journal homepage: https://etj.uotechnology.edu.iq

Synthesis and Characterization of NiP-TiC-SiC Nanocomposite Coating via Electroless Process on Alumina Substrate

Rusul Kh. Abd[a*], **Abbas Kh. Hussein**[b], **Laith K. Abbas**[b]

[a] Polymer and Petrochemical Engineering Dept., Basra University for Oil And Gas – Basra-Iraq
[b] Materials Engineering Dept., University of Technology-Iraq, Alsina'a street, 10066 Baghdad, Iraq.
*Corresponding author Email: rusul.alhamad@buog.edu.iq

HIGHLIGHTS

- The morphology of the coating was changed by the addition of nanoparticles.
- The best contact angle was obtained for the coating prepared at (95°C for 30 minutes).
- Polarization resistance was improved notably for coating produced at (85°C for 60 minutes).

ARTICLE INFO

Handling editor: Mustafa H. Al-Furaiji

Keywords:
Electroless NiP
Coating
Nanoparticles
Contact angle
Corrosion

ABSTRACT

Present-day industrial need high surface engineering quality since it deals with many material properties that are applied in modern applications. Autocatalytic plating of material surfaces enhances their mechanical and chemical properties. This study used electroless plating to create (NiP-TiC-SiC) nanocomposite coatings on alumina ceramic under various time and temperature deposition conditions to get the best performances of nanocomposite coatings. Different coating morphologies have been created, as seen in (FESEM) images. The (EDX) results show that the (NPs) were effectively integrated and that the main elements of the coating are nickel and phosphorus. The (XRD) pattern validates the existence of metallic nickel and the phases (NiP, Ni_2P, and Ni_3P). The hydrophobic properties of the (NiP-TiC-SiC) NCCS generated at (95°C for 30 minutes) increased to (127.26°). The corrosion behavior was studied via the electrochemical method, which was done in the (3.5 wt%) NaCl at (25°C) and the results showed that the addition of (TiC) together with (SiC) nanoparticles shows a significant enhancement in the polarization resistance, the maximum polarization resistance value was obtained for (NiP-TiC-SiC) prepared at (60 minutes 85°C) and it is equal to (56.31419 kΩ.cm).

1. Introduction

Alumina ceramic can be metalized by various techniques including sputtering, vapor deposition, and electroless plating (EL) [1,2]. Due to its ease of use and low cost, the EL deposition procedure was chosen for the current study since it can produce a coating with excellent characteristics. It is an autocatalytic method in which the reduction of metal ions by the oxidation of a reduction agent, and the deposition was done on the materials substrate [3-5]. The substrate is coated while it is dipped in an EL bath, which includes a supply of metal ions, reducing agents, stabilizers, complexing agents, wetting agents, additives, etc [6]. EL (NiP) is frequently employed because of its good corrosion and wear resistance [7-10], it has different benefits, such as uniform plating, and solderability, but it also has some drawbacks, such as worse adhesion and slower plating rate than electroplating[11]. The incorporation of nanoparticles onto a (NiP) matrix from an EL bath led to the form of nano-composite coatings. The enhancement in nanocomposite coating properties depends on the nature of the nanoparticles and their distributions into the matrix [12]. Nanoparticles' sizes range from (1-100 nm), and they exhibit many distinct properties from their parent material because of an increase in the surface area to volume ratio of nanoparticles [13]. There have not been many studies on EL (Ni-P) deposition on alumina substrate; in the year of (2020), K. D. Sameer et al. examined the effect of sensitization and activation settings on the viability of nickel coating on 50 nm alumina particles. A comparison of two activations and sensitizing methods, namely individual and blended activations, had been made when coating particles [14]. While P. Zhang, et al. developed an easy and economical activation method on porous alumina ceramic in the year (2021), They start the EL nickel plating reaction by depositing metallic nickel nanoparticles on the alumina ceramic as a catalytic active core. As a result, the metallic nickel activation process provides a possible activation strategy for EL nickel plating on porous alumina ceramic [10], and R. K. Gupta, et al. produced an experimental study on EL nickel plating on alumina ceramic (2021), and they were successes in producing a uniform and compact coating film [11].

http://doi.org/10.30684/etj.2023.139852.1444
Received 24 May 2023; Received in revised form 09 June 2023; Accepted 25 June 2023; Available online 20 July 2023
2412-0758/University of Technology-Iraq, Baghdad, Iraq

Despite its excellent specifications, alumina cannot be utilized in more widely industrial applications due to its low tensile strength, mechanical unreliability, sensitivity to thermal shocks, and its main shortcoming, brittleness, which results in poor fracture toughness; however, surface metallization has potential to expand its application areas. From the survey of the previous studies, we note that there is not enough study on investigating the possibility of deposited nanocomposite coating on alumina substrate and how the plating period and bath temperature can affect the coating properties, this study aims to develop the best nanocomposite coatings (NCCs) on an alumina substrate by adding (TiC) and (SiC) nanoparticles to the conventional (NiP) bath and plating alumina at various deposition times and temperature in order to get the best performances of EL (NiP-TiC-SiC) nanocomposite coatings.

2. Experimental Work

2.1 Materials

High-purity alumina (99,7%) (C799 aluminum oxide ceramic plate made in China/ shenzhen jinghui industry limited company) samples with dimensions (20 x 20 x 2 mm) were used in this experiment.

The chemicals, sodium hypophosphite purchased from (BDH chemical ltd /England), glycine from (HiMedia Laboratories/India), sodium fluoride, ethanol absolute and hydrochloric acid supplied from (SDFCE sd fine-chem limited/ Mumbai), formaldehyde (panreac QuPimicaSLU C/ Spain), sodium citrate (prolabo/Mexico), sodium acetate (central drug house ltd. Company/India), hydrofluoric acid, and potassium sodium tartrate tetrahydrate purchase from (HIMEDIA laboratories Pvt. Ltd./India), nanoparticles (sic, tic) supplied from china and it characterized in the Nanotechnology and Advanced Materials Research Center/University of Technology.

2.2 Pretreatment and Electroless Plating

(NiP-TiC-SiC) nanocomposite coating on alumina ceramic is summarized using EL (NiP) plating with the addition of (TiC) together with (SiC) nanoparticles under different time and temperature deposition conditions. Pre-treatment, activation, and EL (NiP) plating are the three main steps in the plating process. Pre-treatment includes washing the samples with acetone. The etching process is done by immersing the samples in the mixed aqueous solution of (10%) Hydrofluoric acid and (2 gl-1) Sodium fluoride and stirring for a period of (10 minutes) to generate roughness for making it suitable for adhesion. In the sensitization process, Stannus chloride (SnCl2) (10gl-1) and hydrochloric acid (HCl) (40 ml/l), were stirred for a period of (15 minutes) at room temperature, followed by rinsing with distilled water and then dried. Activation of the surface is the most important step before EL plating. Palladium chloride (PdCl2) (1gml-1) along with (HCl) (10 ml/l) were stirred for a period of (15 minutes). for the activation step. Furthermore, the samples were washed and dried at a temperature of (90^{o}C) for (1 hour). Table 1 mention the process variable of each pretreatment step.

Table 1: The process variable of each pretreatment step for alumina samples

Process	Solution (concentration)	process parameters (temperature, time)
Cleaning	Washing the sample with acetone.	At room temp. for 30 seconds
Etching	(10%) HF and (2 gl^{-1})NaF	For 10 minutes
Sensitization	(10 gl^{-1}) $SnCl_2$ and (40 ml) HCl	15 minutes at room temperature
Activation	Palladium chloride (1 gl^{-1}) $pdCl_2$ and (10 ml) HCl	15 minutes at room temperature
Final step	The samples were washed and dried at a temperature of 90^{o}C for 1 hour	

The plating process is carried out by stirring the palladium-activated alumina samples in a freshly prepared coating bath consisting of nickel sulfate (0.1 M), sodium acetate (0.2 M), sodium citrate (0.16 M), glycine (0.28 M), and Sodium hypophosphite (NaH_2PO_2) (0.36 M) under different plating parameters. The composition of the EL deposition bath can be seen in Table 2. The nano-particles were beta-silicon carbide and titanium carbide.

Table 2: The composition of the electroless deposition bath for alumina samples

Bath Composition	
Nickel sulfate	0.1 M
Sodium hypophosphite	0.63 M
Glycine	0.28 M
Sodium citrate	0.16 M
Nanoparticles SiC and TiC	5 g l^{-1}
Sodium acetate	0.2 M

2.3 Plating Characterization

The nanocomposite coatings were characterized by using different techniques, FESEM (MIRA3 TESCAN, China) (Hv=10 and WD=5) was used to investigate the surface morphology of the coatings the test was done in the University of Tehran/School of Metallurgy and Materials Engineering. EDX provided by "TESCAN Vega II XMU" was employed to analyze the chemical composition of the nanocomposite coatings the test was conducted in the Applied Sciences Department at the University of Technology. XRD (type XRD-7000, Shimadzu) with Cu Kα radiation at (40 kV) and (30 mA) was utilized to characterize the

phase structure of the coatings the test was conducted in the Nanotechnology and Advanced Materials Research Center/University of Technology.

A contact angle meter (Goniometer, Jikan, CAG-10) was used to determine the surface wettability of the nanocomposite coating by applying drops to test samples and capturing pictures of water droplets on the surface. While the corrosion behavior was studied by electrochemical method in (3.5 wt%) NaCl at (25℃), the test was conducted by (SOLARTRON) equipment type with a scan rate of (2 mV s^{-1}) within the potential range of (−250 to +500 mV), both contact angle and corrosion test were done in the university of Tehran/ school of metallurgy and materials engineering.

3. Results and Discussion

3.1 Surface Morphology and Composition of The Coating

The surface morphology of the (NiP) and (NiP-TiC-SiC) NCCs, which were formed at (60 minutes and 85^{0}C), is made clear by the FESEM photos in Figure 1 (A and B). Figure 1(A) Particle-free EL (Ni-P) coatings have nodules that resemble cauliflower, and it is illustrate of an amorphous substance. The surface morphology of the coating is altered by the addition of (2.5 g/l) concentrations of each (TiC) and (SiC). It is obvious that the nucleation of the EL (NiP) nanocomposite coating has been affected by the presence of nanoparticles in the plating bath as shown in Figure 1(B), and that was agreed with the references [15-17].

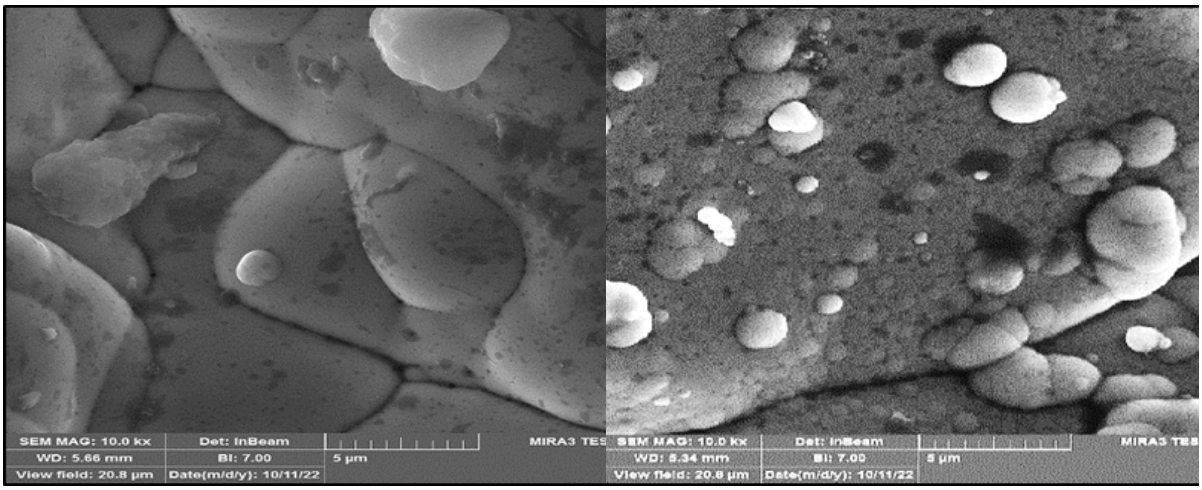

(A) **(B)**

Figure 1: Field emission scanning electron microscope (FESEM) image of the electroless coating prepared at (60 minutes and 85℃) with (A) NiP particle free coating (B) NiP-TiC-SiC nanocomposite coating

The (EDX) spectra of the (Ni-P) and (NiP-TiC-SiC) NCCs prepared at (60 minutes and 85℃) were presented respectively in Figure 2 (A,B) and it is clear that the nanoparticles were successfully incorporated in the matrix.

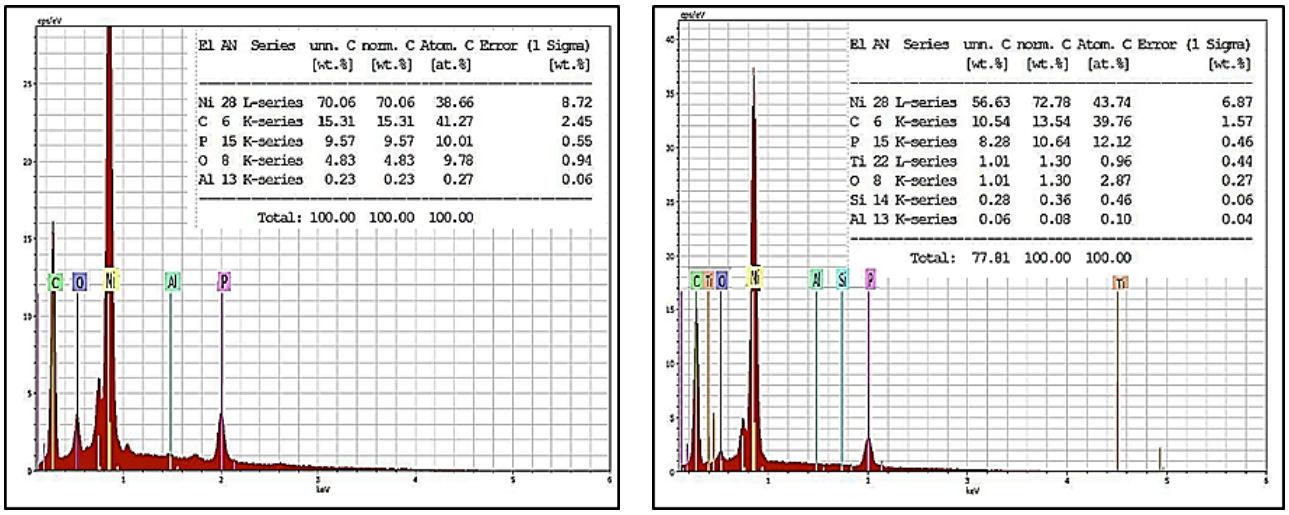

(A) **(B)**

Figure 2: Energy dispersive spectroscopy (EDX) scan spectra of electroless coating at (60 minutes and 85ºC) (A) NiP particle free coating (B) NiP-TiC-SiC nanocomposite coating

Table 3 lists the qualitative analysis of the (NiP) and (NiP-TiC-SiC) obtained by (EDX). The result of (EDX) suggests that the major component in the coating is nickel and shows that the (NPs) were successfully incorporated. The presence of (NPs)

leads to an increase in (Ni) content from (70 wt.%) to (72.78 wt.%) and the phosphorus content increased from (9.57 wt.%) to (10.64 wt.%) respectively.

A dense and evenly distributed nanocomposite coating was obtained when the temperature has been raised and numerous micro-NiP balls was seen on the surface because the plating solution was no longer stable at the highest temperature, and that was agreed with the references [18]. The majority of the substrate is covered as plating time and temperature rise, and no defects like gaps or pinholes are apparent. However, it was noticed that the number and size of (NiP) nodules remain unchanged as the deposition duration increases. The only difference is that some growth of the EL (NiP) matrix on the top of the nanoparticles leads to an increase in the surface roughness of the EL (NiP) nanocomposite coatings, and that was agreed with reference [19]. Figure 3 (A, B,C) depicts the FESEM image of (NiP) nanocomposite coating with both (TiC) and (SiC) NPs prepared at (30 minutes 75°C), (60 minutes 85°C), and (90 minutes 95°C) respectively.

The (EDX) analysis for the (NiP-TiC-SiC) nanocomposite coatings are presented in Figure 4 (A,B,C) deposited at (30 minutes 75°C), (60 minutes 85°C), and (90 minutes 95°C) respectively. The (Ti wt.%) and (SiC wt.%) was utilized to estimate the nanoparticles content because the nanoparticles were the only source of (Ti and Si) in the coating.

The weight percentage of the constituent elements of the nanocomposite coating in the (EDX) data is shown in Table 4. In the case of the (30 minute 75°C) deposition condition, no sufficient coating was obtained, while with increasing deposition time and solution temperature both (Ni wt.%) and (P wt.%) were increased.

(XRD) pattern of (NiP) and (NiP-TiC-SiC) nanocomposite coating prepared at different immersion times and temperatures were shown in Figure 5 (A, B, C, D). Using the previous study data, it is determined that the presented picks correspond to the (012), (104), (110), (113), (024), (116), (018), (300), and (119) of a rhombohedral structure of (α-Al_2O_3) [20]. The sample plating at (30 minutes) immersion time and a temperature of (75°C) exhibited no different broad peak at a (2-Theta) angle (43-50) the nickel peaks, which were confirmed by (EDX).

Table 3: Elemental compositions of nanocomposite coating at (60 minutes and 85°C)

No.	Nanocomposite coating	Ni(wt.%)	P(wt.%)	Ti (wt.%)	Si(wt.%)
A	NiP	70.06	9.57	———	———
B	NiP-TiC-SiC	72.78	10.64	1.30	0.36

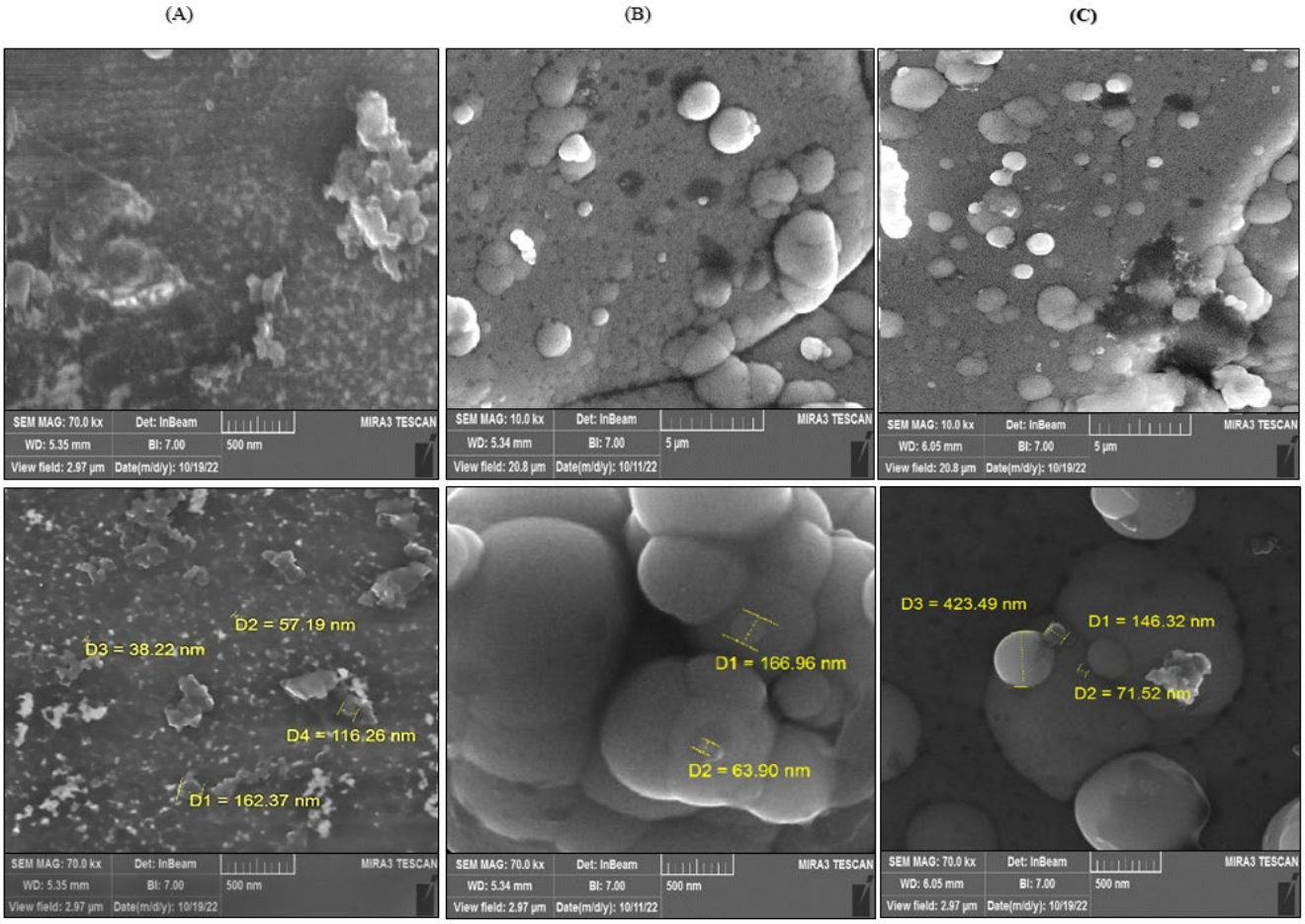

Figure 3: Field emission scanning electron microscope (FESEM) of the nanoparticles of (NiP-TiC-SiC) nanocomposite coating incorporation at (A) 30 minutes 75°C (B) 60 minutes 85°C (C) 90 minutes 95°C

Table 4: Elemental compositions of (NiP-TiC-SiC) nanocomposite coating at different times and temperatures

No.	Electroless deposition time and temp.	Ni (wt.%)	P (wt.%)	Ti (wt.%)	Si (wt.%)
A	30 minutes 75°C	0.43	0.52	9.02	0.87
B	60 minutes 85°C	72.78	10.64	1.30	0.36
C	90 minutes 95°C	76.17	12.08	2.7	0.67

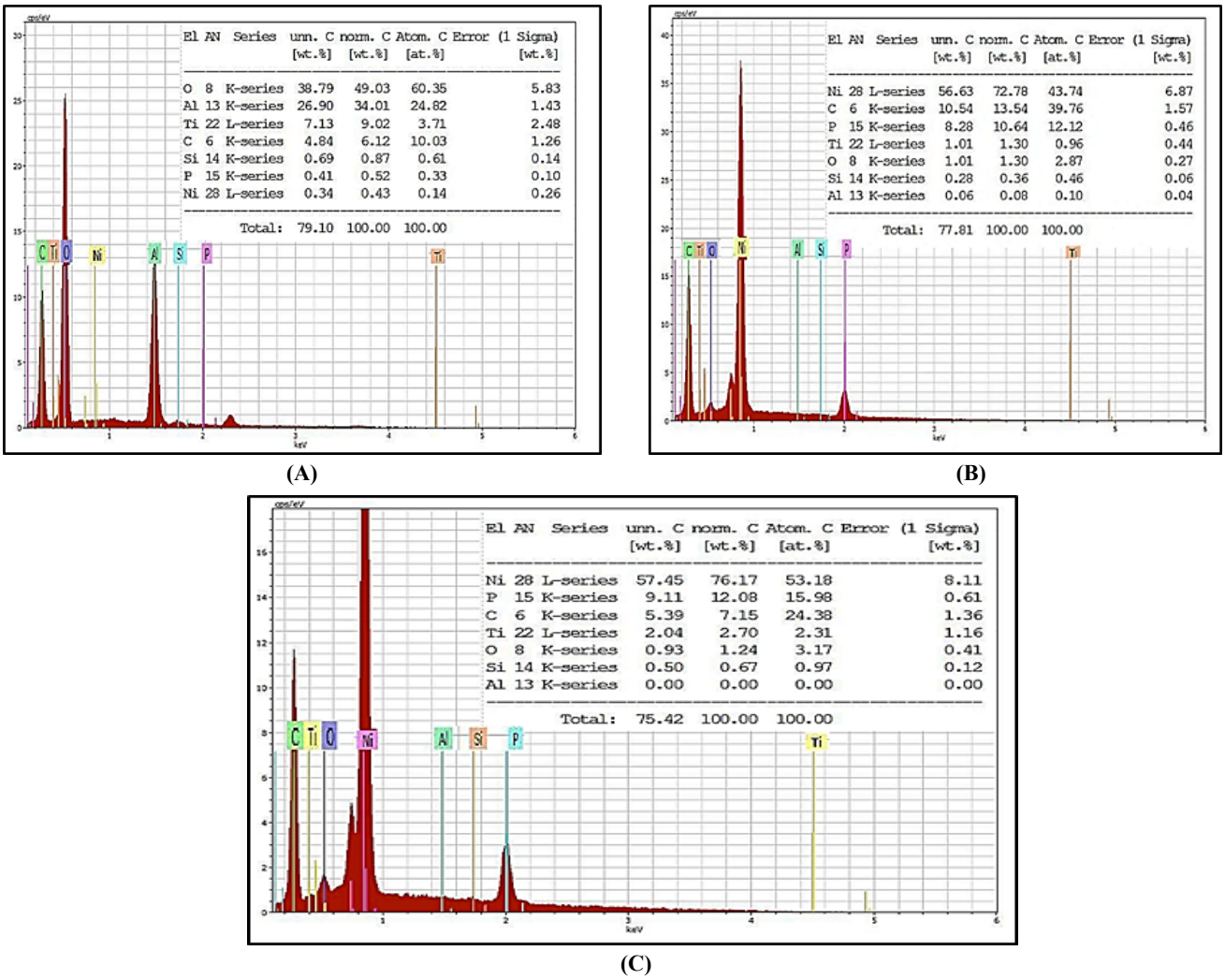

Figure 4: (A), (B), and (C) show the (EDX) spectra of (NiP-TiC-SiC) nanocomposite coating deposited at (30 minutes 75°C), (60 minutes 85°C), and (90 minutes 95°C) respectively

3.2 Contact Angle

Surface wettability is measured using a contact angle meter by applying drops to test samples and capturing pictures of water droplets on the surface of alumina plating by (NiP) and (NiP-TiC-SiC) NCCs using an EL deposition process under different times and temperatures, as shown in Figure 6 (A,B). It was observed that the (NiP-TiC-SiC) nanocomposite coating prepared at (30 minutes 95°C) shows the maximum contact angle value as illustrated in Figure 7. In general, a solid surface is called hydrophilic if the water contact angle is less than (90) degrees, and hydrophobic if the water contact angle is greater than 90 degrees. This is a crucial characteristic for demonstrating effective anticorrosive capabilities. The wettability of the surface was strongly depending on the surface roughness and surface finish, there is a clear relationship between the roughness of the surface and contact angle value, and that was agreed with the reference [21]. The contact angle results show hydrophilic properties on the surface of the coating prepared for a short time and at low temperatures or for a long time and at high plating temperatures. The surface roughness of the finish coating is affected by the plating time; it is normal for the coating to be created in separate locations because deposits frequently develop at multiple locations. With time, the film moves through a diffusion stage distinguished by expanding and merging with the nanoparticles before becoming a solid film. As the deposition time increased, another nodule formed, resulting in high surface roughness due to a large number of nodule protrusions over the surfaces. At the same time, the temperature of the plating bath affects the plating rate, so insufficient plating time or a high plating rate can increase surface roughness and decrease the contact angle.

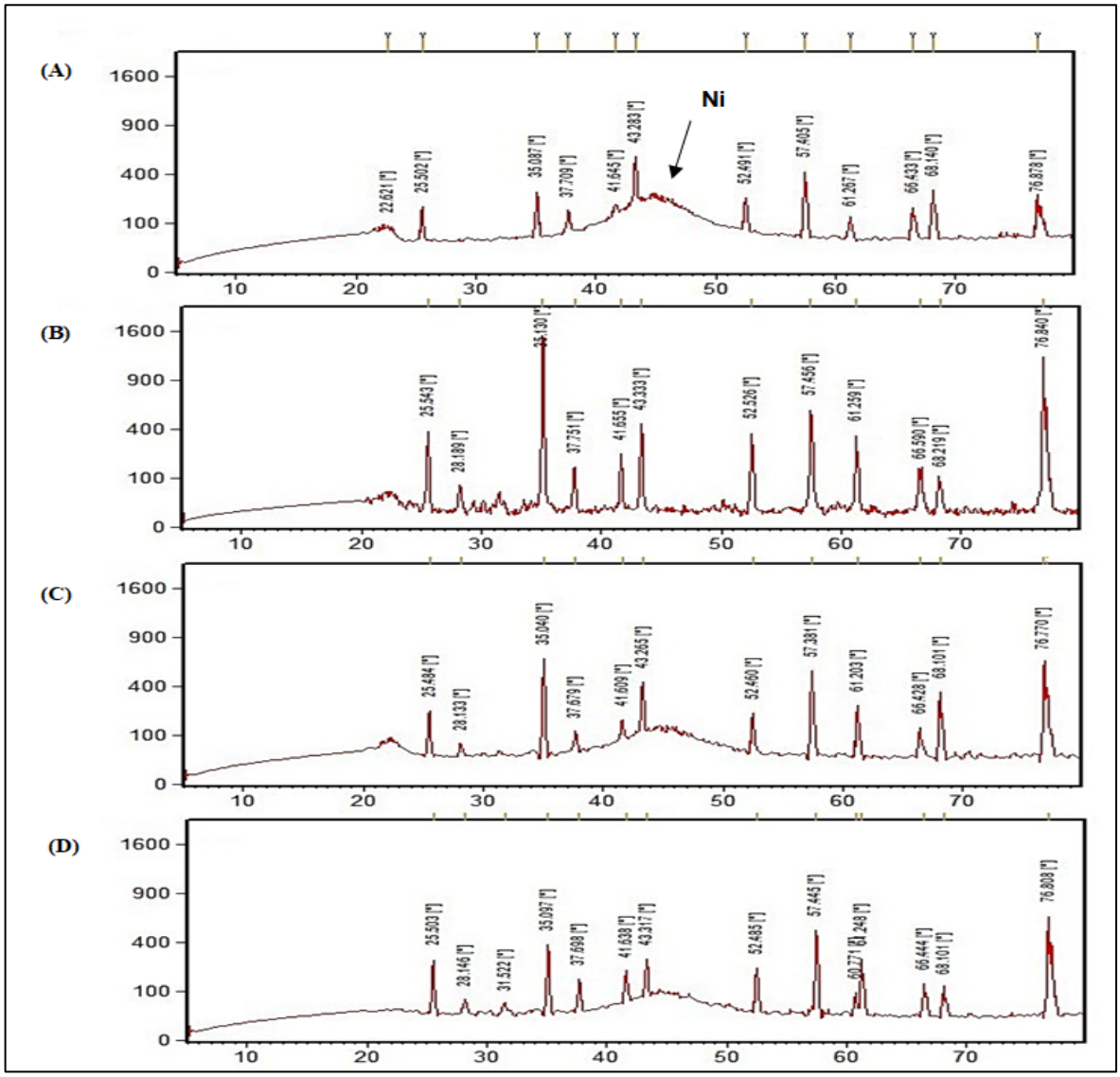

Figure 5: The XRD pattern of (A) NiP, (B) NiP-TiC-SiC prepared at 30 minutes 75℃, (C) NiP-TiC-SiC prepared at 60 minutes 85℃, (D) NiP-TiC-SiC prepared at 90 minutes 95℃

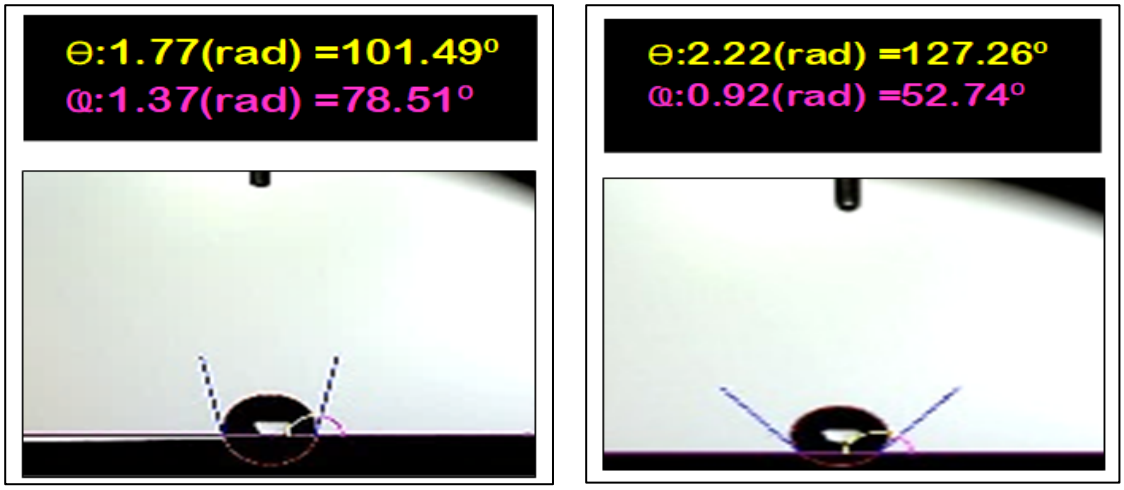

(A) **(B)**

Figure 6: The maximum contact angle measurements of alumina plating by (A) NiP (B) NiP-TiC-SiC, prepared at (30 minutes 95℃)

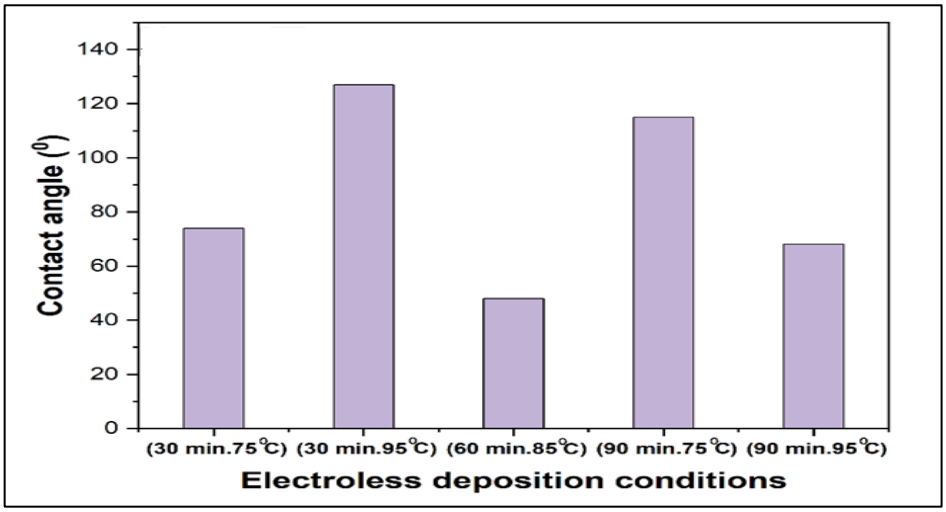

Figure 7: Contact angle results for alumina plating with (NiP-TiC-SiC) nanocomposite coating at different electroless plating conditions

3.3 Corrosion Test

The corrosion resistance of the EL (Ni-P) nanocomposite coating with (TiC) and (SiC) nanoparticles under different deposition conditions was investigated using an electrochemical method in (3.5 wt%) NaCl at (25℃), Figure 8 show the tafel curves (potentiodynamic polarization curves) for the (NiP-TiC-SiC) nanocomposite coating at different EL plating conditions. By extrapolating the linear sections of the anodic and cathodic Tafel lines, researchers were able to measure the samples' corrosion potential (E_{corr}) and current density (I_{corr}), among other electrochemical parameters. These findings are reported along with the cathodic (B_c) and anodic (B_a) tafel slope values in Table 5. The amount of the polarization resistance (Rp) was determined using the Stren-Geary Equation 1 [22] **:**

$$R_p = \frac{B_a.B_c}{2.303 I_{CORR}\,(B_a+B_c)} \quad (1)$$

Since the hypophosphite layer stops nickel from further hydrating in corrosive environments, the hypophosphite layer acts as a protective barrier for nickel, improving the corrosion protection of the (NiP) coatings. With the addition of (NPs), the (NiP) coating's resistivity is greatly increased. As is generally known, (Ti) is a corrosion-resistant metal, which enhances the (NiP) coatings' ability to resist corrosion. The addition of (NPs) makes the (NiP) coatings denser and their porosity reduces, limiting the active sites for corrosion and eliminating direct electrolyte contact with the substrate. In addition, the NiP coatings may be more porous [7]. Adding nanoparticles to the (NiP) matrix has a varied impact on polarization resistance when compared to (NiP-free nanoparticles) [23]. From Figures 9,10 and Table 5, the (NiP-TiC-SiC) nanocomposite coatings at different EL plating conditions show different polarization resistance. And it is clear that the addition of (TiC) together with (SiC) nanoparticles shows a significant enhancement in the polarization resistance of (NiP). The effect of mixing both (TiC) and (SiC) nanoparticles on the enhancement of the polarization resistance of (NCCs) could be explained by the minimization of the size of (NiP) nodules, which served as a physical barrier and prevented chloride ions from diffusing onto the sample surface. The corrosion resistance in the case of deposition at (30 minutes and 85℃) has shown the greatest value, which indicates that the coating is more stable, less soluble, and has fewer porosities.

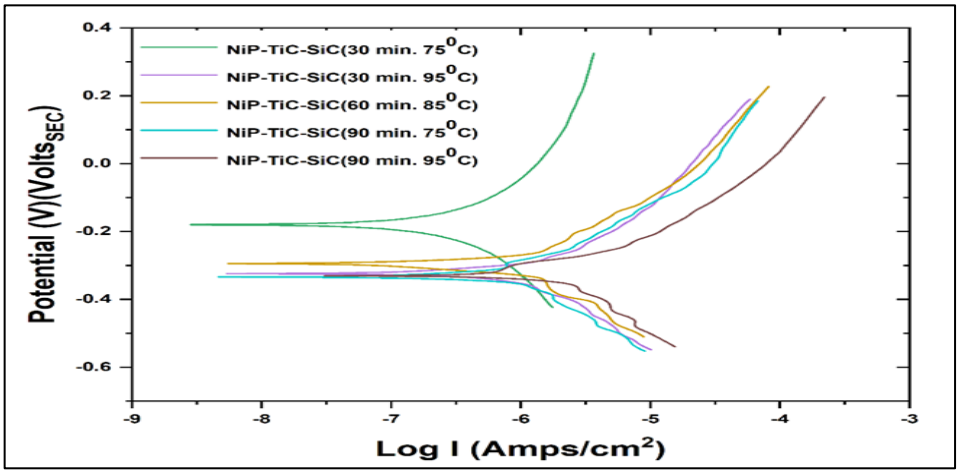

Figure 8: Tafel curves for alumina plating with (NiP-TiC-SiC) nanocomposite coating at different electroless plating conditions immersed in (3.5 wt.%) NaCl solution at (25℃)

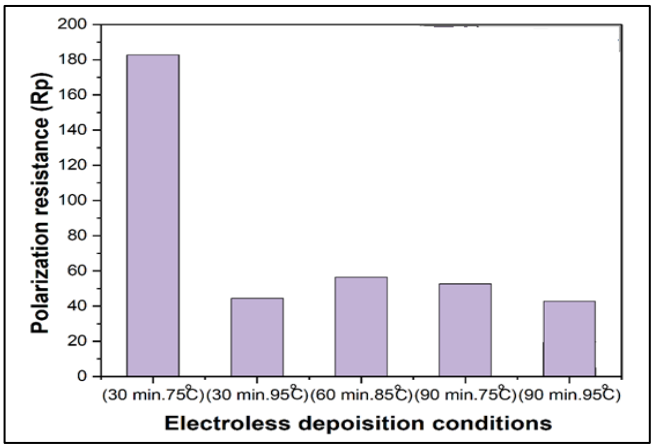

Figure 9: The value of the polarization resistance (Rp) of alumina plating with NiP-TiC- SiC nanocomposite coating at different Electroless plating conditions

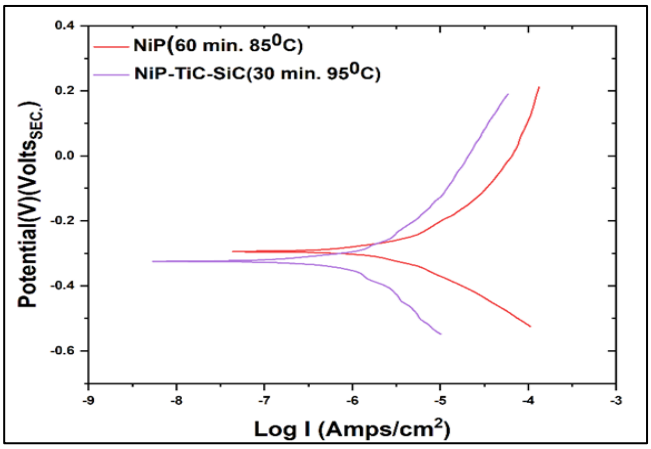

Figure 10: Tafel curves for alumina plating with (NiP and NiP-TiC-SiC) nanocomposite coating at (60 minutes and 85ºC) electroless plating conditions.immersed in (3.5 wt.%) NaCl solution at (25ºC)

Table 5: Tafel fitting results of alumina plating with (NiP-TiC-SiC) nanocomposite coating at different electroless plating conditions that immersed in (3.5 wt.%) NaCl solution at (25°C)

No.	Coating composition	$-E_{corr}$ (mV)	I_{corr} ($\mu A \cdot cm^{-2}$)	B_a (mV/decade)	B_c (mV/decade)	Rp (kΩ. cm)
1	NiP-TiC-SiC (30 min.75°C)	180	0.398107171	330	340	182.6519
2	NiP-TiC-SiC (30 min.95°C)	320	1.071519305	230	210	44.48366
3	NiP-TiC-SiC (60 min.85°C)	290	1.202264435	288	340	56.31419
4	NiP (60 min. 85°C)	298	4.466835922	200	150	8.332192
5	NiP-TiC-SiC (90 min.75°C)	330	0.933254301	200	260	52.59586
6	NiP-TiC-SiC (90 min.95°C)	320	0.361409863	186	47	45.07762

4. Conclusion

The main purpose of this study is to develop the best nanocomposite coating (NCCs) on an alumina substrate by adding (TiC) and (SiC) nanoparticles to the conventional (NiP) plating bath and depositing at various bath temperatures and for various plating period in order to get the best hydrophobic and corrosion resistance performance. The addition of (TiC) and (SiC) nanoparticles to the (NiP) deposition bath changed the morphology of the nanocomposite coating deposited on an alumina substrate; as a result, the best contact angles have been obtained for the electroless (NiP-TiC-SiC) nanocomposite coating prepared at (95°C for 30 minutes), and it is equal to (127.26º). While the (NiP-TiC-SiC) nanocomposite coating produced at (85°C for 60 minutes) exhibits a notable improvement in polarization resistance.

Author contributions

Conceptualization, R. Abd, A. Hussein and L. Abbas; validation, A. Hussein and L. Abbas and R. Abd; investigation, R. Abd; resources, R. Abd; writing—original draft preparation, A. Hussein and L. Abbas; supervision, A. Hussein and L. Abbas; project administration, A. Hussein and L. Abbas. All authors have read and agreed to the published version of the manuscript.

Funding

This research received no specific grant from any funding agency in the public, commercial, or not-for-profit sectors.

Data availability statement

The data that support the findings of this study are available on request from the corresponding author.

Conflicts of interest

The authors declare that there is no conflict of interest.

References

[1] M. Farahmandjou and N. Golabiyan, New pore structure of nano-alumina (Al_2O_3) prepared by sol gel method, J. Ceram. Process. Res., 16 (2015) 237–240.

[2] Y. Yang, W. Tianhe, Y. Tingting, L. Gang, S. Yangshan, C. Xin, M. Liyun and P. Shou, Preparation of a novel TiN/TiNxOy/SiO_2 composite ceramic films on aluminum substrate as a solar selective absorber by magnetron sputtering, J. Alloys Compd., 815 (2020) 152209. https://doi.org/10.1016/j.jallcom.2019.152209

[3] P.D. Garman, J. M. Johnson, V. Talesara, H. Yang, D. Zhang, J. Castro, W. Lu, J. Hwang and L.J. Lee, Silicon Oxycarbide Accelerated Chemical Vapor Deposition of Graphitic Networks on Ceramic Substrates for Thermal Management Enhancement, ACS Appl. Nano Mater., 2 (2019) 452–458. https://doi.org/10.1021/acsanm.8b01998

[4] Y. Wang, Y. H. Xu, Z. Y. Cao, C. Yan, K. Wang, J. J.Chen, S.Y.Cheng and Z. S. Feng, A facile process to manufacture high performance copper layer on ceramic material via biomimetic modification and electroless plating, Composites, Part B: Eng., 157 (2019) 123–130. https://doi.org/10.1016/j.compositesb.2018.08.030

[5] M. M. Shinyar, L. K. Abbas and A. Kh. Hussein, Optimization of mechanical behavior of (Ni-P) nanocomposite coatings using taguchi approach, Int. J. mech. prod. Eng. Rese. Dev., 11 (2021) 99-110.

[6] S. Z. Ali, L. K. Abbas and A. Kh. Hussein, Optimization of Electroless Ni-P, Ni-Cu-P and Ni-Cu-P-TiO_2 Nanocomposite Coatings Microhardness using Taguchi Method, IOP Conf. Ser. Mater. Sci. Eng., 1094 (2021) 012168. https://doi.org/10.1088/1757-899X/1094/1/012168

[7] S. Z. Ali, L. K. Abbas and A. Kh. Hussein, Optimization of Corrosion Resistance for Electroless Nano-Coated Carbon Steel Using Taguchi Approach, Int. J. Mech. Prod., 11 (2021) 397-404.

[8] M. L. Bosko, N. Ferreira, A. Catena, M. Sergio Moreno, J. F. Múnera, and L. Cornaglia, Catalytic behavior of Ru nanoparticles supported on carbon fibers for the ethanol steam reforming reaction, Catal. Commun., 114 (2018) 19–23. https://doi.org/10.1016/j.catcom.2018.05.019

[9] X. Wu, G. Hong, and X. Zhang, Electroless Plating of Graphene Aerogel Fibers for Electrothermal and Electromagnetic Applications, Langmuir, 35 (2019) 3814–3821. https://doi.org/10.1021/acs.langmuir.8b04007

[10] P. Zhang, Z. Lv, X. Liu, G. Xie, and B. Zhang, Electroless nickel plating on alumina ceramic activated by metallic nickel as electrocatalyst for oxygen evolution reaction, Catal. Commun., 149 (2021) 106238. https://doi.org/10.1016/j.catcom.2020.106238

[11] R. K. Gupta, A. Nihore, P. R. Sankar, P. Ganesh, and R. Kaul, An Experimental Study on Electroless Nickel Plating on Alumina Ceramic, Chem. Mater. Eng., 8 (2021) 1–6. https://doi.org/10.13189/cme.2021.080101

[12] M. M. Shinyar, A. Kh. Hussein, and L. K. Abbas, A Desirability Function for Evaluation of Corrosion Behavior for Nanocoated-Steel Using Electroless Technique, Eng. Technol. J., 39 (2021) 946–955. https://doi.org/10.30684/etj.v39i6.2009

[13] A. Kh. Hussein, L. K. Abbas, and W. Hassan, Optimization of Steel Hardness Using Nanofluids Quenchants, Kufa J. Eng., 10 (2019) 29–43. https://doi.org/10.30572/2018/KJE/100103

[14] D. Sameer Kumar, K. Naga Sai Suman, and Y. Kalyana Krishna, Preparation and characterization of electroless ni coated nano alumina powder under different sensitization-activation conditions, Metall. Mater. Eng., 27 (2020) 275–288. https://doi.org/10.30544/467

[15] K. Shahzad, E. M. Fayyad, M. Nawaz, O. Fayyaz, R. A. Shakoor, M.K. Hassan, U. M. Adeel, M. N. Baig, A. Raza, A. M. Abdullah, Corrosion and heat treatment study of electroless nip-ti nanocomposite coatings deposited on hsla steel, Nanomaterials, 10 (2020) 1–19. https://doi.org/10.3390/nano10101932

[16] M. Aliofkhazraei and A. S. H. Makhlouf, Handbook of nanoelectrochemistry: Electrochemical synthesis methods, properties, and characterization techniques, Handb. Nanoelectrochemistry Electrochem. Synth. Methods, Prop. Charact. Tech., pp. 1–1451, 2016, https://doi.org/10.1007/978-3-319-15266-0

[17] P. Narasimman, M. Pushpavanam, and V. M. Periasamy, Synthesis, characterization and comparison of sediment electro-codeposited nickel-micro and nano SiC composites, Appl. Surf. Sci., 258 (2011) 590–598. https://doi.org/10.1016/j.apsusc.2011.08.038

[18] S. A. Xu and C. S. Liang, Effect of deposition time and temperature on the performance of electroless Ni-P coatings, Int. J. Electrochem. Sci., 11 (2016) 8817–8826. https://doi.org/10.20964/2016.10.55

[19] M. Kitiwan and D. Atong, Effects of Porous Alumina Support and Plating Time on Electroless Plating of Palladium Membrane, J. Mater. Sci. Technol., 26 (2010) 1148–1152. https://doi.org/10.1016/S1005-0302(11)60016-9

[20] M. Farahmandjou and N. Golabiyan, New pore structure of nano-alumina (Al_2O_3) prepared by sol gel method, J. Ceram. Process. Res., 16 (2015) 1-4.

[21] D. H. Prajitno, A. Maulana, and D. G. Syarif, Effect of Surface Roughness on Contact Angle Measurement of Nanofluid on Surface of Stainless Steel 304 by Sessile Drop Method, J. Phys. Conf. Ser., 739 (2016). https://doi.org/10.1088/1742-6596/739/1/012029

[22] M. Khodaei and A. M. Gholizadeh, SiC nanoparticles incorporation in electroless NiP-Graphene oxide nanocomposite coatings, Ceram. Int., 47 (2021) 25287–25295. https://doi.org/10.1016/j.ceramint.2021.05.250

[23] E. M. Fayyad, M. K. Hassan, K. Rasool, Kh. A. Mahmoud, A. M.A. Mohamed, G. Jarjoura, Novel electroless deposited corrosion — resistant and anti-bacterial NiP–TiNi nanocomposite coatings, Surf. Coatings Technol., 369 (2019) 323–333.